J. Fluid Mech. (2020), *vol.* 882, A7. © Cambridge University Press 2019
doi:10.1017/jfm.2019.780

Re-entrant history force transition for stick–slip Janus swimmers: mixed Basset and slip-induced memory effects

A. R. Premlata[1] **and Hsien-Hung Wei**[1,†]

[1]Department of Chemical Engineering, National Cheng Kung University, Tainan 701, Taiwan

(Received 9 May 2019; revised 25 July 2019; accepted 19 September 2019)

It is well known that a rigid non-slippery particle in unsteady motion can experience a Basset history force with the signature $1/\delta$ decay due to a Stokes boundary layer of thickness δ. For a uniform slip particle with slip length λ, however, a persistent force plateau can replace the usual Basset decay at δ below the slip–stick transition (SST) point $\delta \sim \lambda$ (Premlata & Wei, *J. Fluid Mech.*, vol. 866, 2019, pp. 431–449). Here we analyse the hydrodynamic force on an oscillating stick–slip Janus particle, showing that it can display unusual history force responses that are of neither the no-slip nor the purely slip type but mixed with both. Solving the oscillatory Stokes flow equation together with a matched asymptotic boundary layer theory, we find that the persistent force plateau seen for a uniform slip particle may be destroyed by the presence of the stick portion of a stick–slip Janus particle. Instead, a $1/\delta$ Basset force of amplitude smaller than the no-slip counterpart will re-emerge to dominate the high frequency viscous force response again. This re-entry Basset force, which occurs only after making a stick patch on a slippery particle, is also found to depend solely on the coverage of the stick face irrespective of the slip length of the slip face. When the stick portion is small, in particular, the re-entry Basset decay will exhibit a slip plateau on its tail, displaying a distinctive re-entrant history force transition prior to the SST. But if changing this tiny stick face to be slippery, no matter how small the slip length is, the re-entry Basset decay will disappear and a constant force plateau will return to dominate the force response again. These unusual force responses arising from mixed stick–slip or non-uniform slip effects may not only provide unique hydrodynamic fingerprints for characterizing heterogeneous particles, but also have potential uses in active manipulation and sorting of these particles.

Key words: low-Reynolds-number flows

1. Introduction

A Janus particle is an anisotropic colloid that has two faces with distinct materials or properties. Because of its bifunctional properties, a Janus particle can serve not only as an active motor or a cargo for facilitating transport, but also as a device for promoting molecular detection and guiding colloidal assembly (Walther

† Email address for correspondence: hhwei@mail.ncku.edu.tw

& Müller 2013). When a particle has both hydrophilic and hydrophobic faces, it becomes a stick–slip Janus particle (SSJP). Hydrodynamically, such a particle has an anisotropic mobility mixed with no-slip and slip influences. So the no-slip and the slip contributions to the hydrodynamic force generally are not additive. For this reason, an SSJP may display quite different hydrodynamic characteristics compared to no-slip and slip particles.

Existing investigations on SSJP are mainly focused on the steady situation (Swan & Khair 2008; Willmott 2008; Boymelgreen & Miloh 2011; Crowdy 2013; Sun *et al.* 2013). However, unsteady effects may be important when one wishes to manipulate stick–slip Janus particles using acoustic forces or employs them to mimic unsteady self-propelled swimmers like micro-organisms. Understanding the unsteady force response for an SSJP might provide useful insights into how to engineer or steer stick–slip Janus particles in these situations. To the best of our knowledge, there has been no prior attempt to analyse this problem until the present work.

In this article, we will analyse the hydrodynamic force on an SSJP moving unsteadily in a viscous fluid. Our efforts will be devoted to looking at how mixed no-slip and slip effects influence the characteristics of the history force. Below we briefly provide the relevant background and explain how the problem is motivated.

When a rigid spherical particle (of radius a) is moving at a time-varying speed $\boldsymbol{U}_p(t)$ under the Stokes flow condition in a viscous fluid (of density ρ and viscosity μ), in addition to the Stokes drag, it can further experience additional viscous force and added mass, represented by the second and third terms, respectively, in the expression of the total hydrodynamic force on the particle (Basset 1888; Landau & Lifshitz 1987),

$$F = -6\pi\mu a\boldsymbol{U}_p(t) - 6\pi\mu a\left(\frac{\rho a^2}{\pi\mu}\right)^{1/2}\int_{-\infty}^{t}\frac{\dot{\boldsymbol{U}}_p(t')}{\sqrt{t-t'}}\,\mathrm{d}t' - \frac{2}{3}\pi\rho a^3\dot{\boldsymbol{U}}_p(t). \tag{1.1}$$

Compared to the added mass which is purely of potential-flow origin, the additional viscous force, termed the Basset force, takes the form of a memory integral to account for the history-dependent viscous drag arising from fluid acceleration/deceleration. If the particle starts from rest and moves instantaneously with a constant speed, the Basset force will decay as $t^{-1/2}$ owing to the same decay of the memory kernel. In fact, the Basset force is exactly the drag force resulting from the viscous stress $\sim \mu\boldsymbol{U}_p/\delta$ across the Stokes boundary layer of thickness $\delta \sim (\nu t)^{1/2}$ (with $\nu = \mu/\rho$ being the kinematic viscosity of the fluid) (Landau & Lifshitz 1987).

Perhaps how the boundary layer influences the hydrodynamic force on a rigid particle can be best revealed by letting the particle oscillate with $\boldsymbol{U}_p(t) = \mathcal{U}_p\mathrm{e}^{-\mathrm{i}\omega t}$ (with ω being the oscillation frequency). The force is (Stokes 1851; Lawrence & Weinbaum 1988)

$$F = -6\pi\mu\mathcal{U}_p a\left(1 + \sqrt{2}\frac{\mathrm{e}^{-\mathrm{i}\pi/4}}{\hat{\delta}} + \frac{2}{9}\frac{\mathrm{e}^{-\mathrm{i}\pi/2}}{\hat{\delta}^2}\right)\mathrm{e}^{-\mathrm{i}\omega t}, \tag{1.2}$$

where $\hat{\delta} = (2\nu/\omega a^2)^{1/2}$ measures the extent of the boundary layer $\delta = (2\nu/\omega)^{1/2}$ relative to the particle radius. As indicated by (1.2), the Basset force has the distinctive amplitude $1/\hat{\delta} \propto \omega^{1/2}$ and phase $\pi/4$ ahead of the particle velocity, whereas the inviscid added mass varies as $1/\hat{\delta}^2 \propto \omega$ with phase $\pi/2$. Because the added mass is not dissipative, at high frequencies the particle motion will be mainly dissipated by the Basset force. It is this reason why the Basset force has a strong influence on the behaviour of an unsteadily swimming micro-organism (Wang & Ardekani 2012).

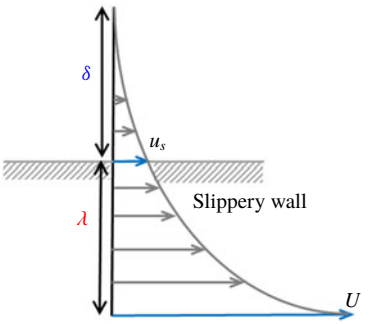

FIGURE 1. (Colour online) Dynamic slip effect in the fluid motion driven by an oscillating slippery plate. Because of slip, the fluid velocity at the plate surface is not the plate speed U but slowed down to $u_s \sim U\delta/(\lambda+\delta)$. The shear stress is thus reduced to $\tau_s \sim \mu u_s/\delta \sim \mu U/(\lambda+\delta)$ and becomes a constant when the boundary layer δ is thinner than the slip length λ.

The same dominance of the Basset force can also happen to the short-term response in particle dynamics when a particle has a transient development in its motion. In particular, when particle inertia is important, the Basset force has been shown crucial to particulate transport in particle-laden flow (Maxey & Riley 1983) and particle dispersion in turbulence (Mei, Adrian & Hanratty 1991). Similar impacts but arising from the non-Basset-like history force can also happen to a rising bubble when it undergoes a rapid shrinkage (Takemura & Magnaudet 2004).

Just like the situation happening to bubbles, while the idea of the history force is rooted in the Stokes boundary layer, the Basset $t^{-1/2}$ kernel is not the sole memory kernel type. Aside from the Basset term, an additional memory term can be introduced through particle asphericity or fluidity (Lawrence & Weinbaum 1986; Galindo & Gerbeth 1993). Unlike the Basset kernel which is singular at $t=0$, such additional memory kernel typically takes the form of $\exp(t/t_0)\mathrm{erfc}((t/t_0)^{1/2})$ which is finite at $t=0$ (Lawrence & Weinbaum 1986), where t_0 is the characteristic time scale. In the case of fluid particles, in particular, these two kernels are working in a somewhat competitive manner. For a fluid droplet, even though the whole memory kernel contains an additional memory kernel, it is still dominated by the $t^{-1/2}$ Basset kernel as $t \to 0$ (Galindo & Gerbeth 1993). But for a gas bubble, the Basset kernel vanishes, whereas the additional memory kernel disappears in the rigid sphere limit (Yang & Leal 1991; Galindo & Gerbeth 1993).

The above features about the memory kernels for fluid particles imply that the difference between the Basset and the non-Basset history forces seems to lie in whether there is fluid slippage on the surface of a particle. Indeed, it has been shown that additional surface slip can significantly modify the characteristics of the history force (Michaelides & Feng 1995; Gatignol 2007). Apparently, surface slip tends to reduce drag, therefore enabling one to describe the situation between the no-slip case and the full-slip bubble case.

And yet, the effects of surface slip are not just simple drag reduction, but have more intriguing impacts on the nature of history force. The reason is that in an unsteady motion, the actual amount of slip a slippery particle perceives is not fixed for a given slip length λ, but constantly changes with the boundary layer thickness δ that also varies with time. As illustrated in figure 1, the situation can be best pictured

by looking at the startup fluid motion driven by a moving slippery plate at speed U. This is essentially the Stokes 1st problem with slip, whose basic features have been demonstrated in detail by Fujioka & Wei (2018). The impacts of slip start from the fact that slip can make the fluid velocity at the surface slow down to $u_s \sim U\delta/(\lambda+\delta)$. This leads the corresponding shear stress to reduce to $\tau_s \sim \mu u_s/\delta \sim \mu U/(\lambda+\delta)$. At the very short time during which δ is much thinner than λ, τ_s remains a constant $\mu U/\lambda$. This constant stress will continue until the slip–stick transition (SST) occurring at $t \sim \lambda^2/\nu$ when $\delta \sim (\nu t)^{1/2}$ grows to the size comparable to λ. After the SST point when δ is thicker than λ, the no-slip result $\mu U/\delta$ reappears.

The simple picture above suggests that slip can completely alter the characteristics of history force. Premlata & Wei (2019) recently re-examined effects of slip on the hydrodynamic force on an oscillating spherical particle, showing that (1.2) is modified to

$$F = -6\pi\mu\mathcal{U}_p a\left[\left(\frac{1+2\hat{\lambda}}{1+3\hat{\lambda}}\right)\left(\frac{1+\sqrt{2}\mathrm{e}^{-\mathrm{i}\pi/4}\dfrac{1}{\hat{\delta}}}{1+\hat{\lambda}(1+3\hat{\lambda})^{-1}\times\sqrt{2}\mathrm{e}^{-\mathrm{i}\pi/4}\dfrac{1}{\hat{\delta}}}\right)+\frac{2}{9}\mathrm{e}^{-\mathrm{i}\pi/2}\frac{1}{\hat{\delta}^2}\right]\mathrm{e}^{-\mathrm{i}\omega t}, \tag{1.3}$$

where $\hat{\lambda}=\lambda/a$ is the dimensionless slip length. Note that the same result (1.3) has been given by early investigations (Albano, Bedeaux & Mazur 1975; Michaelides & Feng 1995) but not fully explored until Premlata & Wei (2019). What Premlata & Wei (2019) found is that in the small $\hat{\delta}$ regime, the viscous part of (1.3) gives a persistent force plateau $6\pi\mu\mathcal{U}_p a^2/\lambda$ at $\hat{\delta}$ below the SST point $\sim\hat{\lambda}$, replacing the usual $1/\hat{\delta}$ Basset decay. In addition, this plateau force becomes in-phase with the particle velocity. Since the constant force plateau can only exist in the presence of slip and get elevated as $\hat{\lambda}$ is decreased, one can conclude that surface slip, no matter how small it is, will make the history force jump from the no-slip $1/\hat{\delta}$ Basset decay down to the constant force plateau in the high frequency regime. The memory kernel is also found to take exactly the same type as that in the bubble case, but is able to attain the constant force plateau as $t\to 0$ and to recover the Basset kernel in the no-slip limit. This is quite distinct from the drop case in which the Basset force still dominates in the short-term viscous force response while an additional memory term is present (Galindo & Gerbeth 1993).

Since purely no-slip and slip particles have completely different history force characteristics and there is no smooth transition between the two in the high frequency or short time regime, this raises a question: how about if a particle consists of both no-slip and slip faces like an SSJP? Specifically, the main question is whether the no-slip Basset force or the slip-induced plateau force dominates the high-frequency or short force response; and more importantly, how these two compete with each other? To answer these questions, it is necessary to analyse the history force response for an SSJP by combining both stick and slip contributions and how the response depends on δ, λ and the partition between the stick and slip portions.

It actually turns out that the history force exerted on an SSJP is neither the no-slip nor the purely slip type but mixed with the two. As will be demonstrated shortly, the detailed force responses can be obtained by analysing the fluid motion around an oscillating SSJP. What we find is that the dominance of the high frequency force plateau seen for a uniform slip particle (Premlata & Wei 2019) will completely disappear due to the presence of the stick part of an SSJP. Instead, a reduced Basset force, which has a smaller amplitude than the no-slip counterpart, will resurface to dictate the viscous force response in the high frequency regime. Since the Basset

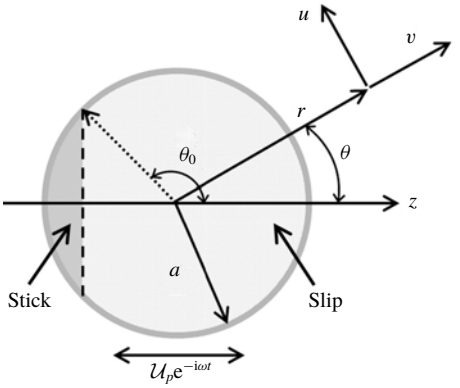

FIGURE 2. Sketch of a spherical stick–slip Janus particle and the coordinate system.

force for a no-slip particle ceases to exist in the $\hat{\delta} \to 0$ limit when the particle becomes uniform slip, but re-emerges with a smaller amplitude when the particle is partially covered by a no-slip surface, we call the latter force the re-entry Basset force to distinguish it from the former. For an SSJP with a tiny stick portion, in particular, the force response can even display a re-entry Basset decay at high frequencies and then level off to a plateau at lower frequencies, showing a distinctive re-entrant history force transition (RHFT) that exists only for an SSJP. Below we demonstrate how we arrive at the above features by solving the oscillatory Stokes flow equation in § 2 and by using the matched asymptotic boundary layer theory in § 3.

2. Hydrodynamics around an oscillating stick–slip Janus particle

Consider the motion of a spherical SSJP of radius a in an incompressible viscous fluid of density ρ and viscosity μ. As depicted in figure 2, the slip part of the particle has polar angle θ_0 in division with the remaining stick part. The particle undergoes an oscillatory translation at speed $\mathcal{U}_p e^{-i\omega t}$ with the peak velocity $\mathcal{U}_p$ and frequency ω. It is more convenient to solve the problem in the translating coordinate system with the origin at the instantaneous centre of the particle. Having length, time, velocity and pressure scaled by a, ω^{-1}, $\mathcal{U}_p$ and $\mu\mathcal{U}_p/a$, respectively, the velocity field $\boldsymbol{v}'$ and pressure p' around the particle are governed by the continuity equation and the unsteady Stokes flow equation,

$$\nabla \cdot \boldsymbol{v}' = 0, \tag{2.1}$$

$$\Omega \boldsymbol{v}'_{t'} = -\nabla p' + \nabla^2 \boldsymbol{v}', \tag{2.2}$$

where $\Omega = \omega a^2/\nu$ is the dimensionless frequency (with $\nu = \mu/\rho$ being the kinematic viscosity). For simplicity, we assume that the particle is moving along its bipolar direction so that the flow field $\boldsymbol{v}' = (u', v')$ can be expressed in terms of the meridional (θ) component u' and the radial (r) component v'. This axisymmetric fluid motion is likely to be the case in steady oscillation because any misalignment of the particle movement from the bipolar direction will cause the particle to rotate until an alignment is achieved.

Because the fluid motion is oscillatory, it is more convenient to solve the problem in the frequency domain by letting $(u', v', p') = (u, v, p)e^{-it'}$. Taking curl for (2.2) to

eliminate pressure with $\nabla \times \nabla p = 0$ and writing the velocity components in terms of the stream function ψ for satisfying (2.1),

$$u = -\frac{1}{r\sin\theta}\frac{\partial \psi}{\partial r}, \quad v = \frac{1}{r^2\sin\theta}\frac{\partial \psi}{\partial \theta}, \tag{2.3a,b}$$

we can transform (2.2) into

$$\mathrm{E}^2(\mathrm{E}^2 - \alpha^2)\psi = 0, \tag{2.4}$$

where $\mathrm{E}^2 = \partial_{rr} + r^{-2}(1-\eta^2)\partial_{\eta\eta}$ with $\eta = \cos\theta$ and $\alpha = (-\mathrm{i}\Omega)^{1/2}$ is the complex Womersley number with $Re\{\alpha\} > 0$.

Boundary conditions are the mixed stick–slip condition at $r = 1$, the impenetrability condition at $r = 1$, and the vanishing velocity condition as $r \to \infty$,

$$u + \sin\theta = \beta(\theta)\left[r\frac{\partial}{\partial r}\left(\frac{u}{r}\right) + \frac{1}{r}\frac{\partial v}{\partial \theta}\right] \quad \text{at } r = 1, \tag{2.5}$$

$$v = \cos\theta \quad \text{at } r = 1, \tag{2.6}$$

$$u, v \to 0 \quad \text{as } r \to \infty. \tag{2.7}$$

In (2.5), $\beta(\theta) = \hat{\lambda}$ for the slip face and 0 otherwise, where $\hat{\lambda} = \lambda/a$ is the dimensionless slip length.

As in Lawrence & Weinbaum (1986), the solution of (2.4) that satisfies (2.7) takes the form

$$\psi = \sum_{n=2}^{\infty}[A_n H_n(r) + B_n R_n(r)]G_n(\eta), \tag{2.8}$$

where $H_n(r) = r^{-n+1}$, $R_n(r) = r^{1/2}\mathrm{K}_{n-1/2}(\alpha r)$ with $\mathrm{K}_{n-1/2}$ being modified Bessel functions of second kind, and G_n the Gegenbauer functions of degree $-1/2$. The coefficients A_n and B_n are determined by substituting (2.8) into (2.5) and (2.6) and applying the orthogonality $\int_{-1}^{1} G_m(\eta)G_n(\eta)/(1-\eta^2)\,\mathrm{d}\eta = \delta_{mn}C_n$ over these two boundary conditions, where δ_{mn} is the Kronecker delta and $C_n = 2/n(n-1)(2n-1)$. From (2.6), we can express B_n in terms of A_n as $B_n = \delta_{2n} - A_n H_n(1)/R_n(1)$. Applying (2.5) and eliminating B_n, we arrive at the following infinite system of linear equations (via m) for A_n:

$$\sum_{n=2}^{\infty}\{\delta_{mn}C_n\mathcal{G}_n + \mathcal{L}_{mn}d_n\}A_n = 2\{C_2\delta_{2m} + \mathcal{L}_{m2}\} - C_m j_m \delta_{2m} - \sum_{n=2}^{\infty}\mathcal{L}_{mn}e_n\delta_{2n}, \tag{2.9}$$

where

$$\left.\begin{aligned} &\mathcal{G}_n = H_n'(1) - \frac{H_n(1)}{R_n(1)}R_n'(1), \quad d_n = 2H_n'(1) - H_n''(1) - \frac{H_n(1)}{R_n(1)}\{2R_n'(1) - R_n''(1)\}, \\ &\mathcal{L}_{mn} = \int_{-1}^{1}\frac{G_m(\eta)G_n(\eta)\beta(\eta)}{1-\eta^2}\,\mathrm{d}\eta, \quad e_n = \frac{1}{R_n(1)}\{2R_n'(1) - R_n''(1)\}, \quad j_n = \frac{R_n'(1)}{R_n(1)}. \end{aligned}\right\} \tag{2.10}$$

After solving (2.9), the force on the particle can be readily determined as $F = \hat{F}\mathrm{e}^{-\mathrm{i}\omega t}$ with

$$\hat{F} = \mu\mathcal{U}_p a(-2\pi A_2 + V_p)\alpha^2, \tag{2.11}$$

where $V_p = 4\pi/3$ is the dimensionless particle volume. In this work we are mainly concerned with the viscous part of $\hat{F}$ after subtracting the added mass contribution $-6\pi\mu\mathcal{U}_p a \times (\alpha^2/9)$,

$$\hat{F}^{vis} = 6\pi\mu\mathcal{U}_p a(-A_2 + 1) \times (\alpha^2/3). \tag{2.12}$$

We have verified analytically that when β is constant, (2.12) is reduced to the viscous part of (1.3). For given α, θ_0 and $\hat{\lambda}$, equation (2.9) can be solved by truncation and matrix inversion. In the present work, convergent results can be obtained by retaining 100 terms in the solution (2.8).

Figure 3(*a*) plots the viscous force amplitude $|\hat{F}^{vis}|$ against $\hat{\delta} = (2/\Omega)^{1/2}$ for an SSJP with a slip hemisphere ($\theta_0 = 90°$). Several features can be immediately observed. First, for a given value of $\hat{\lambda}$ the high frequency force plateau seen for the uniform slip case disappears. Instead, a Basset $1/\hat{\delta}$ decay emerges and dominates the force response in the small $\hat{\delta}$ regime. This is the re-entry Basset force after a slippery particle is partially covered by a stick cap. Second, all the curves with different values of $\hat{\lambda}$ approach towards the same re-entry Basset asymptote as $\hat{\delta} \to 0$ (see the inset). Third, the amplitude of such an asymptote is slightly smaller than that of the no-slip Basset force. The corresponding phase $\phi^{vis} = \tan^{-1}(\mathrm{Im}(\hat{F}^{vis})/\mathrm{Re}(\hat{F}^{vis}))$ also approaches the Basset value $-\pi/4$ as $\hat{\delta} \to 0$, as indicated by figure 3(*b*). Note that there is a phase jump between the no-slip case ($\phi_{vis} = -\pi/4$) and the uniform slip case ($\phi_{vis} = 0$). So returning from $\phi_{vis} = 0$ for a completely slip sphere to $\phi_{vis} = -\pi/4$ for an SSJP is also an indication of the re-entry Basset force seen in the latter.

The appearance of the re-entry Basset decay between the no-slip Basset decay and the uniform slip force plateau seen in figure 3(*a*) implies that there must be a competition between no-slip and slip memory effects, depending on the stick–slip partition measured by θ_0. Figure 4(*a*) plots the viscous force responses when the stick portion is gradually reduced by increasing θ_0. We find that when the stick portion is shrunk, not only will the re-entry Basset $1/\hat{\delta}$ decay reduce its amplitude, but also a slip plateau will start to re-appear on the tail of the re-entry Basset decay. When the stick portion becomes tiny such as that of the $\theta_0 = 150°$ case, in particular, the force response shows the coexistence of a re-entry Basset decay and a slip plateau. This clearly signifies an RHFT, featured with two transition points: (i) the RHFT point when the re-entry Basset decay starts to level off towards the slip plateau, and (ii) the SST point $\hat{\delta} \sim \hat{\lambda}$ around which the slip plateau starts to decrease towards the usual Basset decay. We should clarify that either transition represents a gradual change from one force response to another, so the corresponding point should be understood as a 'crossover' between two different force responses. Interestingly, if a Janus particle is made of two slip surfaces, the re-entry Basset decay will disappear and the slip force plateau will return to dominate the viscous force response in the small $\hat{\delta}$ regime, as also revealed by figure 4(*a*). The disappearance of the re-entry Basset force in the small $\hat{\delta}$ regime is accompanied by a jump of the phase $\phi^{vis}(\hat{\delta} \to 0)$ from $-\pi/4$ to zero when the stick–slip case changes to the slip–slip case, as shown in figure 4(*b*).

3. Matched asymptotic boundary layer theory

To explain the results shown in figures 3 and 4 as well as to see how RHFT occurs, we develop a matched asymptotic boundary layer theory for capturing the force response in the small δ regime when Ω is large. Similar to previous studies by Wang (1965) and Riley (1966), we let $\epsilon = 1/\Omega^{1/2} = \hat{\delta}/\sqrt{2}$ be the small parameter to expand the flow fields outside and inside the boundary layer as follows.

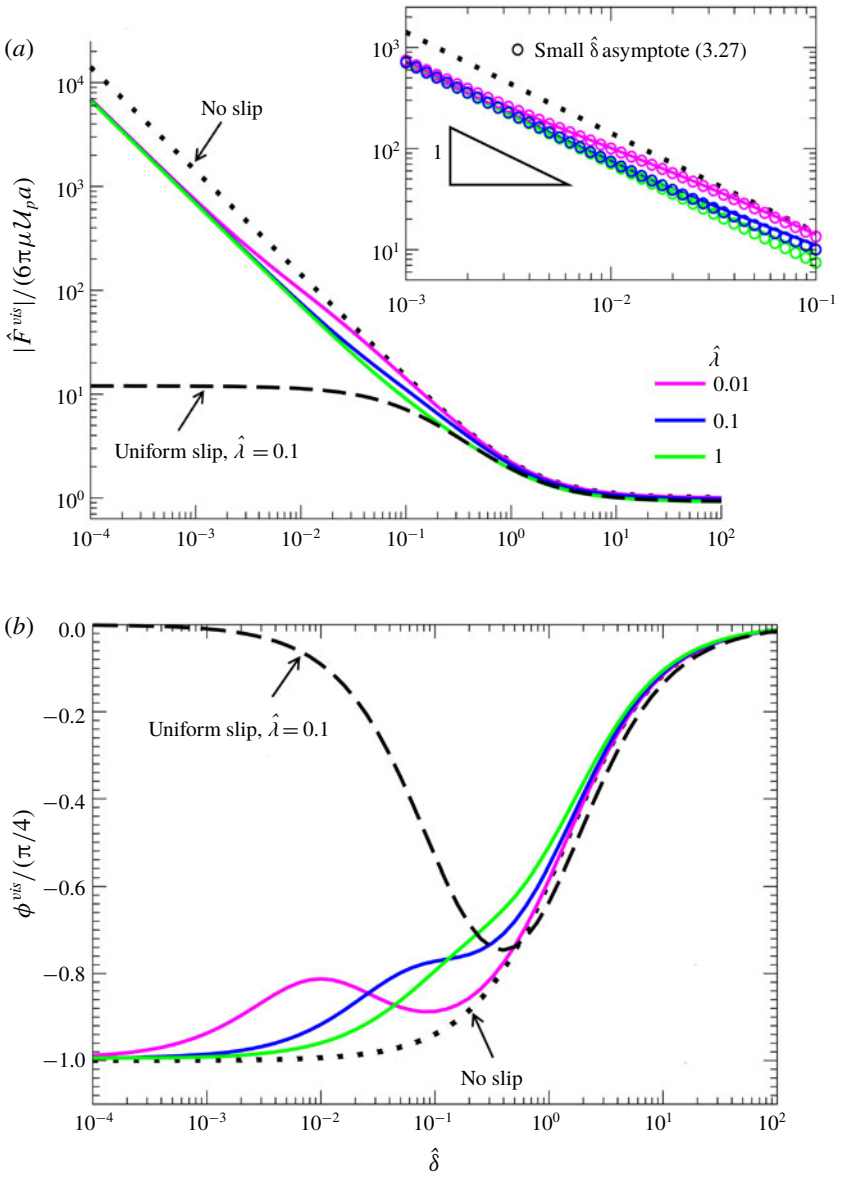

FIGURE 3. (Colour online) (*a*) Plot of the calculated viscous force amplitude $|\hat{F}^{vis}|/(6\pi\mu\mathcal{U}_p a)$ (using (2.12)) against $\hat{\delta}$ for an SSJP with a slip hemisphere ($\theta_0 = 90°$), showing that all the curves with different values of $\hat{\lambda}$ approach towards the same re-entry Basset $1/\hat{\delta}$ asymptote (3.27) as $\hat{\delta} \to 0$ (see the inset). (*b*) Plot of the corresponding phase ϕ^{vis} as a function of $\hat{\delta}$, showing that ϕ^{vis} also approaches $-\pi/4$ as $\hat{\delta} \to 0$.

3.1. *Outer inviscid core region*

In the outer core regime, we let $\boldsymbol{\mathcal{V}} = (U, V)$ and P stand for the velocity field and pressure, respectively, and expand them as

$$\boldsymbol{\mathcal{V}} = \boldsymbol{\mathcal{V}}_0 + \epsilon \boldsymbol{\mathcal{V}}_1 + O(\epsilon^2), \tag{3.1}$$

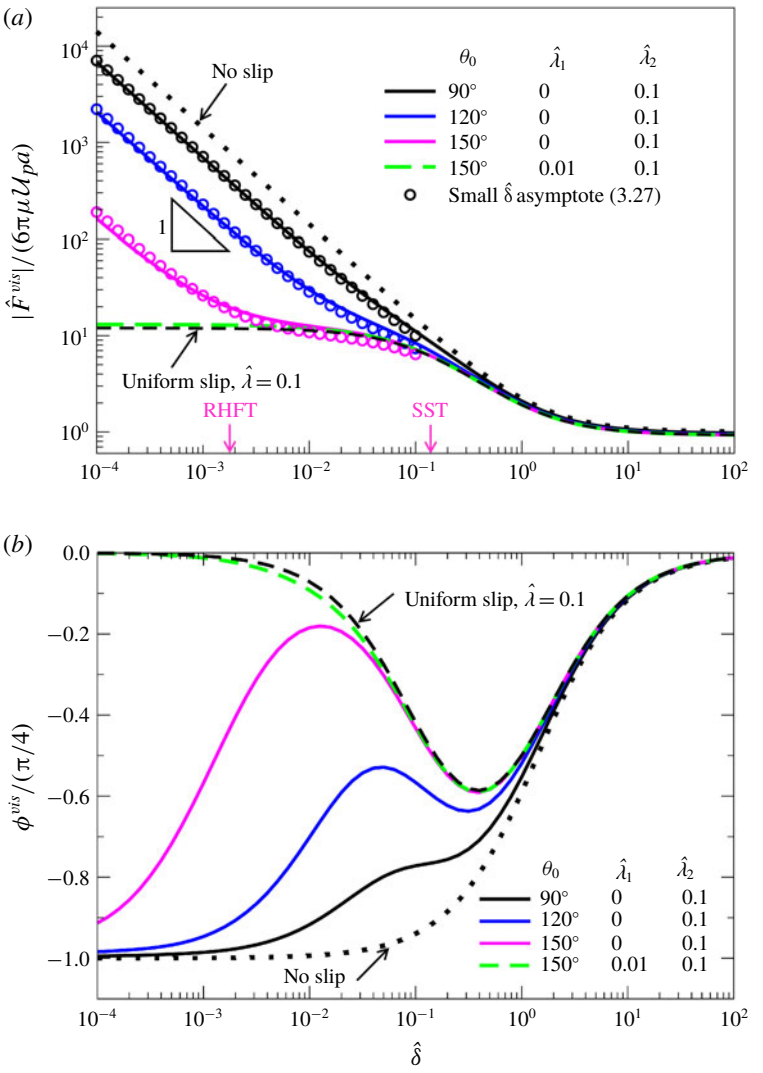

FIGURE 4. (Colour online) (*a*) History force transition between the re-entry Basset decay and the slip plateau can be more clearly revealed from the viscous force response when the stick portion of an SSJP is gradually reduced. When the stick portion becomes tiny such as that of $\theta_0 = 150°$ case, the prevailing re-entry Basset decay can exhibit a slip plateau on its tail in the small $\hat{\delta}$ regime (see pink solid line), showing two transition points: RHFT and SST points given by (3.30) and (3.28), respectively. For a slip–slip Janus particle, however, the re-entry Basset decay will disappear and a constant force plateau will return to dominate the force response again (see green dashed line). (*b*) A jump of the phase $\phi^{vis}(\hat{\delta} \to 0)$ from $-\pi/4$ to zero when the stick–slip case changes to the slip–slip case.

$$P = \epsilon^{-2} P_0 + \epsilon^{-1} P_1 + O(\epsilon^0). \tag{3.2}$$

Substituting the above into (2.1) and (2.2), we find that at both $O(\epsilon^0)$ and $O(\epsilon^1)$ the flows are inviscid and irrotational, governed by $\nabla \cdot \boldsymbol{\mathcal{V}}_n = 0$ and $-\mathrm{i}\boldsymbol{\mathcal{V}}_n = -\nabla P_n$. So the

flows can be solved using $\nabla^2\phi_n = 0$ with $\boldsymbol{\mathcal{V}}_n = \boldsymbol{\nabla}\phi_n$, giving the velocity and pressure distributions at each order as follows.

$O(\epsilon^0)$:

$$U_0 = -(\mathcal{A}/r^3)\sin\theta, \tag{3.3}$$
$$V_0 = -2(\mathcal{A}/r^3)\cos\theta, \tag{3.4}$$
$$P_0 = \mathrm{i}(\mathcal{A}/r^2)\cos\theta. \tag{3.5}$$

$O(\epsilon)$:

$$U_1 = (\mathcal{A}_1/r^3)\sin\theta, \tag{3.6}$$
$$V_1 = -2(\mathcal{A}_1/r^3)\cos\theta, \tag{3.7}$$
$$P_1 = \mathrm{i}(\mathcal{A}_1/r^2)\cos\theta. \tag{3.8}$$

Here the coefficients $\mathcal{A}$ and $\mathcal{A}_1$ will be determined through matching to the solution in the inner boundary layer region.

3.2. *Inner boundary layer region*

For the inner boundary layer region where viscous effects are important, we stretch the radial coordinate as $r = 1 + \epsilon y$ and expand the flow variables as

$$u = u_0 + \epsilon u_1 + O(\epsilon^2), \tag{3.9}$$
$$v = \cos\theta + \epsilon v_0 + O(\epsilon^2), \tag{3.10}$$
$$p = \epsilon^{-2}p_0 + \epsilon^{-1}p_1 + O(\epsilon^0). \tag{3.11}$$

Substituting the above into (2.1) and (2.2), at leading order the equations are

$$\partial_y v_0 + \frac{1}{\sin\theta}\frac{\partial}{\partial\theta}(u_0\sin\theta) = 0, \tag{3.12}$$
$$-\mathrm{i}u_0 = -\partial_\theta p_0 + \partial_{yy}u_0, \tag{3.13}$$
$$\partial_y p_0 = 0. \tag{3.14}$$

Because of (3.14), p_0 remains constant across the boundary layer. Matching $\epsilon^{-2}p_0$ to the outer pressure $\epsilon^{-2}P_0(r \to 1^+)$ with (3.5), we can determine p_0 as

$$p_0 = \mathrm{i}\mathcal{A}\cos\theta. \tag{3.15}$$

Next, we substitute (3.15) into (3.13) to determine u_0 using the mixed stick-slip boundary condition at $y = 0$,

$$u_0 + \sin\theta = (\beta(\theta)/\epsilon)\partial_y u_0. \tag{3.16}$$

In (3.16) we retain both the no-slip part (on the left-hand side) and the slip part (on the right-hand side) in the present analysis, just like those in the Stokes 1st problem (Fujioka & Wei 2018). The reasons are twofold. First, because the fluid is dragging along with the particle through the driving velocity $\sin\theta$ along the particle surface, impacts of slip can only be brought by having the slip term at least balanced to the $\sin\theta$ term in the no-slip part, especially when the amount of slip $\hat{\lambda} = \lambda/a$ varies. Second, to capture the non-trivial transition from the no-slip response to the slip

response, it is more convenient to retain both parts in (3.16). Specifically, since the effective slip coefficient $\beta(\theta)/\epsilon$ can be either small or large depending on the polar angle θ_0 that divides the stick and the slip faces for an SSJP, it is necessary to keep the no-slip part in (3.16) so that one can see how its effects compete with the slip part's as θ_0 varies.

With (3.15) and (3.16), we solve (3.13) to determine u_0 as

$$u_0 = (\mathcal{A} - 1)\sin\theta[\mathrm{e}^{-ky}g(\theta) - 1] - \sin\theta, \tag{3.17}$$

where $k = \mathrm{e}^{-\mathrm{i}\pi/4}$ and $g(\theta) = (1 + k\beta(\theta)/\epsilon)^{-1}$ is a piecewise continuous function because of $\beta(\theta)$ in (2.5). Strictly speaking, the present boundary layer analysis is valid only if $|\mathrm{d}\beta/\mathrm{d}\theta| \ll \epsilon^{-1}$. As will be shown later in the force expression (3.25), since we will be only concerned with the first two harmonic contributions from $g(\theta)$, effects of the piecewise continuity, which contribute to higher harmonics, will not matter. Substituting (3.17) into (3.12), we can solve for v_0 with $v_0(y = 0) = 0$,

$$v_0 = k^{-1}(\mathcal{A} - 1)(\mathrm{e}^{-ky} - 1)\frac{1}{\sin\theta}\frac{\partial}{\partial\theta}(g(\theta)\sin^2\theta) + 2\mathcal{A}y\cos\theta. \tag{3.18}$$

At the next order, we only need to determine the pressure which again is a function of θ only because $\partial_y p_1 = 0$. Similar to (3.15), matching $\epsilon^{-1}p_1$ to the outer pressure $\epsilon^{-2}P_1(r \to 1^+)$ with (3.8) gives

$$p_1 = \mathrm{i}\mathcal{A}_1\cos\theta. \tag{3.19}$$

3.3. *Matching*

To determine the coefficients $\mathcal{A}$ and $\mathcal{A}_1$ we match the radial velocities of the outer and the inner regions,

$$\lim_{r\to 1}(V_0 + \epsilon V_1 + \cdots) \Longleftrightarrow \lim_{y\to\infty}(\cos\theta + \epsilon v_0 + \cdots) \quad \text{as } \epsilon \to 0. \tag{3.20}$$

This is equivalent to the matching between the outer and the inner stream functions (Riley 1966). Substituting (3.4) and (3.7) into the left-hand side of (3.20) and taking an expansion in ϵ, we arrive at

$$(V_0 + \epsilon V_1 + \cdots)_{r\to 1} = [-2\mathcal{A} + \epsilon(-2\mathcal{A}_1 + 6\mathcal{A}y) + \cdots]\cos\theta + \cdots. \tag{3.21}$$

As for the right-hand side of (3.20), substituting (3.18) into it gives

$$(\cos\theta + \epsilon v_0 + \cdots)_{y\to\infty} = \cos\theta - \epsilon k^{-1}(\mathcal{A} - 1)\frac{1}{\sin\theta}\frac{\partial}{\partial\theta}(g(\theta)\sin^2\theta) + 2\mathcal{A}\epsilon y\cos\theta. \tag{3.22}$$

Expanding $g(\theta)\sin^2\theta$ in terms of the Gegenbauer functions $G_n(\cos\theta)$ of degree $-1/2$ and matching the terms in (3.21) to those in (3.22), we find

$$\mathcal{A} = -1/2, \quad \mathcal{A}_1 = (3/2k)(\mathcal{A} - 1)\int_{-1}^{1} g(\eta)G_2(\eta)\,\mathrm{d}\eta. \tag{3.23}$$

3.4. *Hydrodynamic force*

The amplitude of the hydrodynamic force on the particle can be evaluated according to

$$\frac{\hat{F}}{\mu \mathcal{U}_p a} = 2\pi \int_0^{\pi} (\sigma_{rr} \cos\theta - \sigma_{r\theta} \sin\theta)_{y=0} \sin\theta \, \mathrm{d}\theta. \tag{3.24}$$

The normal stress $\sigma_{rr}(y=0) = -p(y=0) + 2(\partial v/\partial r)_{y=0}$ is dominated by the pressure term until $O(\epsilon^{-1})$ because of (3.11) and $(\partial v/\partial r)_{y=0} \sim O(\epsilon^0)$. With (3.15) and (3.19), it can be evaluated as $\sigma_{rr}(y=0) = \mathrm{i}\mathcal{A} \cos\theta \epsilon^{-2} + \mathrm{i}\mathcal{A}_1 \cos\theta \epsilon^{-1} + O(\epsilon^0)$. With (3.17), the tangential stress can be evaluated as $\sigma_{r\theta}(y=0) = \epsilon^{-1}(\partial u_0/\partial y)_{y=0} + O(\epsilon^0) = -\epsilon^{-1} k \sin\theta g(\theta)(\mathcal{A} - 1) + O(\epsilon^0)$. Combining the above stresses into (3.24) together with (3.23), we obtain the force amplitude as

$$\frac{\hat{F}}{-6\pi\mu\mathcal{U}_p a} = \frac{1}{9\epsilon^2} \mathrm{e}^{-\mathrm{i}\pi/2} + \frac{1}{\epsilon} \mathrm{e}^{-\mathrm{i}\pi/4} \left(g_0 - \frac{1}{5} g_2 \right) + O(\epsilon^0). \tag{3.25}$$

Here the ϵ^{-2} term is the added mass, and the ϵ^{-1} term is the viscous force with $g_0 = (1/2) \int_{-1}^{1} g(\eta) \mathcal{P}_0(\eta) \, \mathrm{d}\eta$ and $g_2 = (5/2) \int_{-1}^{1} g(\eta) \mathcal{P}_2(\eta) \, \mathrm{d}\eta$ representing the monopole and the quadrupole contributions, respectively, where $\mathcal{P}_n$ are the Legendre functions.

For the slip–slip case with $\beta(\eta) = \hat{\lambda}_1 + \mathcal{H}(\eta - \eta_0)(\hat{\lambda}_2 - \hat{\lambda}_1)$ where $\mathcal{H}$ is the Heaviside step function, the viscous part of (3.25) becomes

$$\frac{\hat{F}^{vis}}{-6\pi\mu\mathcal{U}_p a} = \frac{\mathrm{e}^{-\mathrm{i}\pi/4}}{\epsilon \Delta} \left[1 + \frac{k}{2\epsilon} \left\{ (\hat{\lambda}_1 + \hat{\lambda}_2) + \eta_0 \left(1 - \frac{1}{2}(\eta_0 - 1)(\eta_0 + 1) \right) (\hat{\lambda}_2 - \hat{\lambda}_1) \right\} \right] + O(\epsilon^0), \tag{3.26}$$

where $\Delta = (1 + k\hat{\lambda}_1/\epsilon)(1 + k\hat{\lambda}_2/\epsilon)$. As $\epsilon \to 0$, equation (3.26) gives a constant force plateau having zero phase shift. In the case of $\eta_0 = 0$ (hemisphere), the plateau value is $1/\hat{\lambda}_{eff}$ where the effective slip length $\hat{\lambda}_{eff} = 2/(\hat{\lambda}_1^{-1} + \hat{\lambda}_2^{-1})$ is exactly the harmonic mean of $\hat{\lambda}_1$ and $\hat{\lambda}_2$.

For the stick–slip case with $\hat{\lambda}_1 = 0$, equation (3.26) is reduced to

$$\frac{\hat{F}^{vis}}{-6\pi\mu\mathcal{U}_p a} = \frac{1}{\epsilon} \mathrm{e}^{-\mathrm{i}\pi/4} \frac{1}{(1 + k\hat{\lambda}_2/\epsilon)} \left[1 + \frac{k\hat{\lambda}_2}{\epsilon} (\eta_0 + 1)^2 \mathcal{C} \right] + O(\epsilon^0), \tag{3.27}$$

where $\mathcal{C} = (2 - \eta_0)/4$. The small $\hat{\delta}$ force responses seen in figures 3 and 4 can be excellently captured by the asymptotic result (3.27). On the right-hand side of (3.27), the first term is the reduced force due to slip, which yields a constant force plateau $1/\hat{\lambda}_2$ at ϵ below the SST point at $|k|\hat{\lambda}_2/\epsilon \approx 1$,

$$\epsilon_{\mathrm{SST}} \approx \hat{\lambda}_2. \tag{3.28}$$

The second term arises from the stick part. This term outweighs the first as $\epsilon \to 0$, giving the re-entry Basset force,

$$\frac{\hat{F}_{\mathrm{RB}}}{-6\pi\mu\mathcal{U}_p a} = \epsilon^{-1} \mathrm{e}^{-\mathrm{i}\pi/4} (\eta_0 + 1)^2 \mathcal{C}, \tag{3.29}$$

which depends solely on the coverage of the stick face but not on the slip length $\hat{\lambda}_2$. This re-entry Basset force will start to decrease towards the slip plateau when ϵ is increased to the RHFT point at $|k|\hat{\lambda}_2(\eta_0+1)^2C/\epsilon \approx 1$ in (3.27),

$$\epsilon_{\mathrm{RHFT}} \approx \hat{\lambda}_2(\eta_0+1)^2\mathcal{C} \approx (\eta_0+1)^2\mathcal{C}\epsilon_{\mathrm{SST}}. \tag{3.30}$$

As indicated by (3.30), if the stick face is small (i.e. η_0 is close to -1), ϵ_{RHFT} will become well separated from ϵ_{SST} given by (3.28), as can be clearly seen from the $\theta_0 = 150^\circ$ curve in figure 4(*a*). But if changing this small stick face to be slippery, no matter how small $\hat{\lambda}_1$ is, RHFT will disappear and the constant force plateau will return to dominate the force response again, as indicated by (3.26).

Re-entrant history force transition can be best revealed from (3.27) in the memory integral form if the particle undergoes a transient movement. In this case, we can express the particle velocity as a Fourier integral, convert (3.27) in terms of the Laplace variable s with $-\mathrm{i}\omega \to s$, and then carry out an inverse Laplace transform. If the particle starts from rest, i.e. $\mathcal{U}_p = 0$ for $t \leqslant 0$, and moves at $\mathcal{U}_p = \mathcal{U}_p(t)$ for $t > 0$, equation (3.27) can be written as the following memory integral:

$$\frac{F^{vis}(t)}{-6\pi\mu a} = \int_0^t \frac{\mathrm{d}\mathcal{U}_p(\tau)}{\mathrm{d}\tau} M(t-\tau)\,\mathrm{d}\tau, \tag{3.31}$$

with the memory kernel

$$M(t) = \frac{1}{\hat{\lambda}_2}\exp\left(\frac{t}{t_{\mathrm{SST}}}\right)\mathrm{erfc}\left(\left(\frac{t}{t_{\mathrm{SST}}}\right)^{1/2}\right)(1-(\eta_0+1)^2\mathcal{C}) + \frac{(\eta_0+1)^2\mathcal{C}}{\sqrt{\pi}}\left(\frac{t}{t_v}\right)^{-1/2} + \cdots. \tag{3.32}$$

Here $t_v = a^2/\nu$ is the viscous diffusion time. The slip–stick transition time, t_{SST}, is

$$t_{\mathrm{SST}} = \hat{\lambda}_2^2 t_v = \lambda_2^2/\nu, \tag{3.33}$$

which is shorter than t_v for $\hat{\lambda}_2 < 1$. As clearly revealed by (3.32), $M(t)$ consists of two contributions: the slip kernel and the Basset kernel, characterized by t_{SST} and t_v, respectively. For $\eta_0 = -1$, it recovers the uniform slip result (Premlata & Wei 2019). If $\mathcal{U}_p(t) = \mathcal{U}_0$ (const.), equation (3.31) with $\hat{\lambda}_2 < 1$ has the following short-term response for $t/t_v \ll 1$,

$$\frac{F^{vis}(t)}{-6\pi\mu\mathcal{U}_0 a} = \frac{\mathcal{C}(\eta_0+1)^2}{\sqrt{\pi}}\left(\frac{t}{t_v}\right)^{-1/2} + \frac{1-\mathcal{C}(\eta_0+1)^2}{\hat{\lambda}_2}\left(1-\frac{2}{\sqrt{\pi}}\left(\frac{t}{t_{\mathrm{SST}}}\right)^{1/2}\right) + O(t/t_v). \tag{3.34}$$

The leading contribution is the re-entry Basset $t^{-1/2}$ decay. The next is the $O(t^0)$ slip plateau with a $t^{1/2}$ tail due to SST. Re-entrant history force transition occurs when the former is decreased to the latter when the boundary layer of thickness $\delta \sim (\nu t)^{1/2}$ grows to the size at time

$$t_{\mathrm{RHFT}} \approx \left(\frac{\mathcal{C}(\eta_0+1)^2}{\sqrt{\pi}(1-\mathcal{C}(\eta_0+1)^2)}\right)^2 t_{\mathrm{SST}}. \tag{3.35}$$

So t_{RHFT} becomes quite sensitive to the coverage of the stick face, (η_0+1). If the stick portion is small, RHFT will occur at time $\sim(\eta_0+1)^4 t_{\mathrm{SST}}$ much earlier than SST upon the start of the particle movement. If such a particle undergoes an oscillatory motion, the RHFT frequency corresponding to (3.35) is $\omega_{\mathrm{RHFT}} \sim (\eta_0+1)^{-4}\omega_{\mathrm{SST}}$ much higher than the SST frequency $\omega_{\mathrm{SST}} \sim \nu/\lambda_2^2$ corresponding to (3.33).

4. Concluding remarks

We have demonstrated that an SSJP can display unusual history force responses that are of neither the no-slip nor the purely slip type but mixed with both. We find that the stick portion of an SSJP, no matter how small it is, will always render a Basset force to exhibit $1/\hat{\delta}$ or $t^{-1/2}$ decay in the high frequency or short time regime but of amplitude smaller than that of a no-slip particle. This is the re-entry Basset force because it not only replaces the constant force plateau seen for a slippery particle (Premlata & Wei 2019) but also re-emerges when a slippery particle is patched with a no-slip face. In the case where the stick portion is small, in particular, the re-entry Basset decay will be further accompanied by a slip plateau at a lower frequency or longer time, displaying an RHFT prior to the SST. These unusual force responses only occur to stick–slip Janus particles and are very distinct from those for drops and bubbles (Galindo & Gerbeth 1993; Magnaudet & Legendre 1998). As these force responses are very sensitive to the frequency of the prescribed oscillatory motion, one may be able to utilize them to characterize heterogeneous particles or to perform hydrodynamic sorting of these particles. Alternatively, because how much the stick face covers an SSJP and the amount of slip on the slip face can strongly influence the behaviour of the re-entry Basset force in competition with the slip force plateau, this may offer an advantage for controlling the motion of an SSJP via selecting a proper stick–slip partition. This may be in particular useful to the design of an SSJP if one would like to employ it as a self-propelled swimmer.

Experimentally, the mixed history force responses may be realized by having an SSJP propelled by an acoustic force at frequency ω typically ranging from 100 kHz to 10 MHz (Laurell, Petersson & Nilsson 2007). Consider an SSJP of radius $a \sim 10$ μm and let it undergo an oscillatory translation at the peak velocity $\mathcal{U}_p \sim 10$ μm s^{-1} in water (of $\rho = 1$ g cm^{-3} and $\mu = 10^{-2}$ g cm^{-1} s^{-1}). At frequencies lower than the viscous damping frequency $\omega_\nu = \nu/2\pi a^2 \sim 10^3$ Hz (with $\nu = \mu/\rho$ being the kinematic viscosity), the particle can experience a steady Stokes drag $F_{Stokes} = 6\pi\mu\mathcal{U}_p a \approx 2$ pN. Suppose the slip length is $\lambda \sim 1$ μm, taken as 10 % of the particle radius. The force plateau $F_{plateau} = F_{Stokes}(a/\lambda) \approx 20$ pN may appear at ω higher than the SST frequency $\omega_{\mathrm{SSF}} \sim \nu/2\pi\lambda^2 \sim 10^5$ Hz according to (3.28). The re-entry Basset force $F_{RB} \sim F_{Stokes}(\omega/\omega_\nu)^{1/2}(\eta_0+1)^2$ according to (3.29). For an SSJP with a slip hemisphere (of $2\theta_0 = 180^\circ$ or $\eta_0 = 0$), there is no plateau in the force response (see figure 3*a*). The F_{RB} for this case will be at least $10F_{Stokes} \approx 20$ pN at ω higher than ω_{SSF}. But if F_{RB} starts to show a tail with a slower decay rate as occurring to an SSJP having a small stick cap of angle $2 \times (180 - \theta_0) = 120^\circ$ or $\eta_0 = -1/2$ (see figure 4*a*), F_{RB} can only be seen if ω is raised to the RHFT frequency $\omega_{\mathrm{RHFT}} \sim (\eta_0+1)^{-4}\omega_{\mathrm{SSF}} \sim 10^6$ Hz or higher. The above estimates can also be used to design an acoustically powered microswimmer made by an SSJP for controlling its motion according to a, λ, ω and η_0.

Acknowledgement

This work was supported by the Ministry of Science and Technology of Taiwan under the grant MOST 107-2811-E-006-010 of H.-H.W.

REFERENCES

ALBANO, A. M., BEDEAUX, D. & MAZUR, P. 1975 On the motion of a sphere with arbitrary slip in a viscous incompressible fluid. *Physica* A **80**, 89–97.

BASSET, A. B. 1888 On the motion of a sphere in a viscous liquid. *Phil. Trans. R. Soc. Lond.* A **179**, 43–63.

BOYMELGREEN, A. M. & MILOH, T. 2011 A theoretical study of induced-charge dipolophoresis of ideally polarizable asymmetrically slipping Janus particles. *Phys. Fluids* **23** (7), 072007.

CROWDY, D. G. 2013 Exact solutions for cylindrical slip–stick Janus swimmers in Stokes flow. *J. Fluid Mech.* **719**, R2.

FUJIOKA, H. & WEI, H.-H. 2018 Letter: new boundary layer structures due to strong wall slippage. *Phys. Fluids* **30** (12), 121702.

GALINDO, V. & GERBETH, G. 1993 A note on the force on an accelerating spherical drop at low-Reynolds number. *Phys. Fluids* A **5**, 3290–3292.

GATIGNOL, R. 2007 On the history term of Boussinesq–Basset when the viscous fluid slips on the particle. *C. R. Méc.* **335** (9-10), 606–616.

LANDAU, L. D. & LIFSHITZ, E. M. 1987 *Fluid Mechanics*, 2nd edn. Pergamon.

LAURELL, T., PETERSSON, F. & NILSSON, A. 2007 Chip integrated strategies for acoustic separation and manipulation of cells and particles. *Chem. Soc. Rev.* **36** (3), 492–506.

LAWRENCE, C. J. & WEINBAUM, S. 1986 The force on an axisymmetric body in linearized, time-dependent motion: a new memory term. *J. Fluid Mech.* **171**, 209–218.

LAWRENCE, C. J. & WEINBAUM, S. 1988 The unsteady force on a body at low Reynolds number; the axisymmetric motion of a spheroid. *J. Fluid Mech.* **189**, 463–489.

MAGNAUDET, J. & LEGENDRE, D. 1998 The viscous drag force on a spherical bubble with a time-dependent radius. *Phys. Fluids* **10** (3), 550–554.

MAXEY, M. R. & RILEY, J. J. 1983 Equation of motion for a small rigid sphere in a nonuniform flow. *Phys. Fluids* **26** (4), 883–889.

MEI, R., ADRIAN, R. J. & HANRATTY, T. J. 1991 Particle dispersion in isotropic turbulence under Stokes drag and Basset force with gravitational settling. *J. Fluid Mech.* **225**, 481–495.

MICHAELIDES, E. E. & FENG, Z.-G. 1995 The equation of motion of a small viscous sphere in an unsteady flow with interface slip. *Intl J. Multiphase Flow* **21** (2), 315–321.

PREMLATA, A. R. & WEI, H.-H. 2019 The Basset problem with dynamic slip: slip-induced memory effect and slip–stick transition. *J. Fluid Mech.* **866**, 431–449.

RILEY, N. 1966 On a sphere oscillating in a viscous fluid. *Q. J. Mech. Appl. Maths.* **19** (4), 461–472.

STOKES, G. G. 1851 On the effect of the internal friction of fluids on the motion of pendulums. *Trans. Camb. Phil. Soc.* **9**, 8–106.

SUN, Q., KLASEBOER, E., KHOO, B. C. & CHAN, D. Y. C. 2013 Stokesian dynamics of pill-shaped Janus particles with stick and slip boundary conditions. *Phys. Rev.* E **87** (4), 043009.

SWAN, J. W. & KHAIR, A. S. 2008 On the hydrodynamics of slip–stick spheres. *J. Fluid Mech.* **606**, 115–132.

TAKEMURA, F. & MAGNAUDET, J. 2004 The history force on a rapidly shrinking bubble rising at finite Reynolds number. *Phys. Fluids* **16** (9), 3247–3255.

WALTHER, A. & MÜLLER, A. H. E. 2013 Janus particles: synthesis, self-assembly, physical properties, and applications. *Chem. Rev.* **113** (7), 5194–5261.

WANG, C.-Y. 1965 The flow field induced by an oscillating sphere. *J. Sound Vib.* **2** (3), 257–269.

WANG, S. & ARDEKANI, A. M. 2012 Unsteady swimming of small organisms. *J. Fluid Mech.* **702**, 286–297.

WILLMOTT, G. 2008 Dynamics of a sphere with inhomogeneous slip boundary conditions in Stokes flow. *Phys. Rev.* E **77** (5), 055302.

YANG, S.-M. & LEAL, L. G. 1991 A note on memory-integral contributions to the force on an accelerating spherical drop at low Reynolds number. *Phys. Fluids* A **3** (7), 1822–1824.